the plant journal

SEB SOCIETY FOR EXPERIMENTAL BIOLOGY

The Plant Journal (2024) **120,** 1343–1357 doi: 10.1111/tpj.17053

Deep learning to capture leaf shape in plant images: Validation by geometric morphometrics

Ladislav Hodač[1,*], Kevin Karbstein[1], Lara Kösters[1], Michael Rzanny[1], Hans Christian Wittich[2], David Boho[2], David Šubrt[3], Patrick Mäder[2,4,5] and Jana Wäldchen[1,4]

[1]*Department Biogeochemical Integration, Max Planck Institute for Biogeochemistry, Jena, Germany,*
[2]*Data-intensive Systems and Visualization Group, Technische Universität Ilmenau, Ilmenau, Germany,*
[3]*Faculty of Science, Jan Evangelista Purkyně University in Ústí nad Labem, Ústí nad Labem, Czech Republic,*
[4]*German Centre for Integrative Biodiversity Research – iDiv (Halle-Jena-Leipzig), Leipzig, Germany, and*
[5]*Faculty of Biological Sciences, Friedrich Schiller University Jena, Jena, Germany*

Received 17 May 2024; revised 26 August 2024; accepted 18 September 2024; published online 9 October 2024.
*For correspondence (e-mail lhodac@outlook.com).

SUMMARY

Plant leaves play a pivotal role in automated species identification using deep learning (DL). However, achieving reproducible capture of leaf variation remains challenging due to the inherent "black box" problem of DL models. To evaluate the effectiveness of DL in capturing leaf shape, we used geometric morphometrics (GM), an emerging component of eXplainable Artificial Intelligence (XAI) toolkits. We photographed *Ranunculus auricomus* leaves directly *in situ* and after herbarization. From these corresponding leaf images, we automatically extracted DL features using a neural network and digitized leaf shapes using GM. The association between the extracted DL features and GM shapes was then evaluated using dimension reduction and covariation models. DL features facilitated the clustering of leaf images by source populations in both *in situ* and herbarized leaf image datasets, and certain DL features were significantly associated with biological leaf shape variation as inferred by GM. DL features also enabled leaf classification into morpho-phylogenomic groups within the intricate *R. auricomus* species complex. We demonstrated that simple *in situ* leaf imaging and DL reproducibly captured leaf shape variation at the population level, while combining this approach with GM provided key insights into the shape information extracted from images by computer vision, a necessary prerequisite for reliable automated plant phenotyping.

Keywords: deep learning, leaf images, phenotypic variation, eXplainable AI, geometric morphometrics, *Ranunculus auricomus*, smartphone imaging *in situ*.

INTRODUCTION

A morphometric approach to capture plant phenotypes

The study of phenotypic variation in natural plant populations is a crucial component of ecological, evolutionary, and conservation research. It provides information on the variability of specific traits, which are important for studying responses to both abiotic and biotic environmental conditions, as well as for discriminating between individuals, populations, or species (Karbstein et al., 2020; Stuessy, 2009). Plant vegetative organs like leaves are widely used due to their immense morphological diversity, which encodes both taxon-specific traits and environmentally influenced phenotypic plasticity (Hodac et al., 2023; Wu et al., 2023). Accurate and biologically meaningful measures of phenotypic similarity are provided by geometric morphometrics (GM), a statistical method that captures unbiased shape information derived from biologically homologous points called landmarks (Bookstein, 1997). Landmarks provide a more straightforward measure of shape differences than pixel-based methods such as segmentation or edge detection. GM allows prior biological knowledge (e.g., assignment to genetic groups or geographically isolated populations) to be incorporated into the analyses by selecting appropriate landmarks, ensuring that the shape analysis is consistent with the underlying biology of the morphological structures under study (Petrović et al., 2015; Qi et al., 2024; Reich et al., 2020). The GM approach, including multivariate statistics, models shape changes that effectively discriminate between taxa (Klingenberg, 2013; Zelditch et al., 2012). Additionally, GM provides visually comprehensive and statistically quantifiable representations of shape variation within datasets, while remaining insensitive to variations in background,

illumination, contrast, and other imaging conditions that can affect segmentation and edge detection techniques.

Computer vision approach—deep learning

With immense technical progress and increasing availability of images, deep learning (DL) models, particularly convolutional neural networks (CNNs), have gained significant attention in automatic plant identification in recent years, achieving high levels of classification accuracy (Borowiec et al., 2022; Mäder et al., 2021). The superiority of DL features over traditional morphometric measurements has been demonstrated for several plant benchmark datasets (Beikmohammadi et al., 2022; Saleem et al., 2019; Tan et al., 2020). CNNs also outperform traditional machine learning classifiers (e.g., K-Nearest Neighbors/KNN) based on biological features such as leaf shape and color (Kayhan, 2022; Wäldchen et al., 2018). The power of CNNs lies in learning leaf features directly from raw input data, including hierarchical transformations from lower to higher levels of abstraction (Lee et al., 2017). Thus, plant classification can now be measured based on image descriptors (i.e., DL features) automatically extracted from images (Rzanny et al., 2022). However, although DL models accurately classify taxa, their decision-making process remains a black box to the human observer (Mostafa et al., 2023). As a result, we cannot determine the specific biological feature that distinguishes the classified taxa. An answer can be provided by comparing DL features (AI) with GM shapes (quantitative shape analysis), an approach to eXplainable AI (XAI). XAI aims to understand how DL models make decisions (Gunning & Aha, 2019; Holzinger et al., 2022). Shedding light on the black-box nature of plant taxa classification can pave the way for DL applications in integrative plant taxonomy, which requires biologically meaningful and reproducible comparisons between taxa, as well as automated species phenotyping. As a consequence of the growing interest in automatic DL-based plant classification and its poorly understood biological interpretability, eXplainable Artificial Intelligence (XAI) has emerged as a new field in this domain (de Benito Fernández et al., 2023; Holzinger et al., 2022; Li et al., 2022; Samek et al., 2021). New XAI approaches are constantly being developed, for example, activation maximization has been used to interpret the decisions made by CNNs in plant disease classification (Toda & Okura, 2019). Feature map visualization has identified specific regions within leaf images that influence the CNN classification of different *Quercus* species (Lee et al., 2017). Grad-CAM is a widely used XAI technique in plant science that generates heat maps highlighting the regions of plant images crucial for classification (Borraz-Martínez et al., 2022; de Benito Fernández et al., 2023; Noviandy et al., 2023), with alternatives such as LIME or SHAP (Mahin et al., 2022; Nahiduzzaman et al., 2023; Paul et al., 2023). Dimension reduction techniques such as UMAP and t-SNE are also part of the XAI toolkit, as they help explore the global and local structures within the high-dimensional datasets generated by CNN features (Tan et al., 2022). Despite the progress in XAI, several knowledge gaps remain. A key question is how well the features prioritized by CNNs in plant image classification correspond to actual biological variation in shape, and how this variation can be quantified. Recent studies, such as a comparison of plant seed and fruit stone classification using CNN and outline-based GM, have shed light on the potential of GM as an XAI tool (Bonhomme et al., 2023). While GM combined with machine learning is well established in fields such as zoology, anthropology, and medicine (Bellin et al., 2022; de Lima et al., 2024; Le et al., 2020; Rodrigues et al., 2022; Sano & Kawabata, 2023; Wöber et al., 2021, 2022), its application in plant science is still an emerging discipline.

Model plant group

To study leaf shape variation in the context of XAI, we focus here on the *Ranunculus auricomus* species complex (Figure 1a), chosen as a model group due to its diverse leaf shapes resulting from hybridization, polyploidy, and apomixis (asexuality). Recent studies have unraveled the origins of this morphological diversity, illustrating the intricate interplay of hybrid derivatives from sexual ancestors (Hodac et al., 2018, 2023; Karbstein et al., 2020). The combination of phylogenomic analyses with GM has been crucial in elucidating morphological variation among genetic lineages, and thus in redefining sexual progenitor species (Karbstein et al., 2020). Europe-wide sampling of sexual species and asexual lineages and analysis of their genomic structures has delineated three major genetic clusters aligned with distinct morphological characteristics (Karbstein et al., 2022). For simplicity, these three major morpho-phylogenomic clusters will be referred to as "morpho-phylo-groups" throughout the text. The three morpho-phylo-groups (abbreviated as "C," "E," "N") are distinguished (among other traits) by basal leaf morphology, which exhibits high variability at multiple systematic levels, including populations and even individual plants. Leaf morphological variation in apomictic/asexual lineages of the *R. auricomus* species complex has been linked to parental subgenome contributions and climatic factors (Hodac et al., 2023).

Research questions

Plant leaves are ideal model organs for studying the synergy between computer vision and quantitative morphology, particularly GM, due to their inherent morphological diversity, phenotypic plasticity, well-defined geometric properties, and ease and affordability of image acquisition. Our goal is to utilize DL to automatically extract features from images of identical leaves photographed both *in situ* and after herbarization (Figure 1a). We will then compare

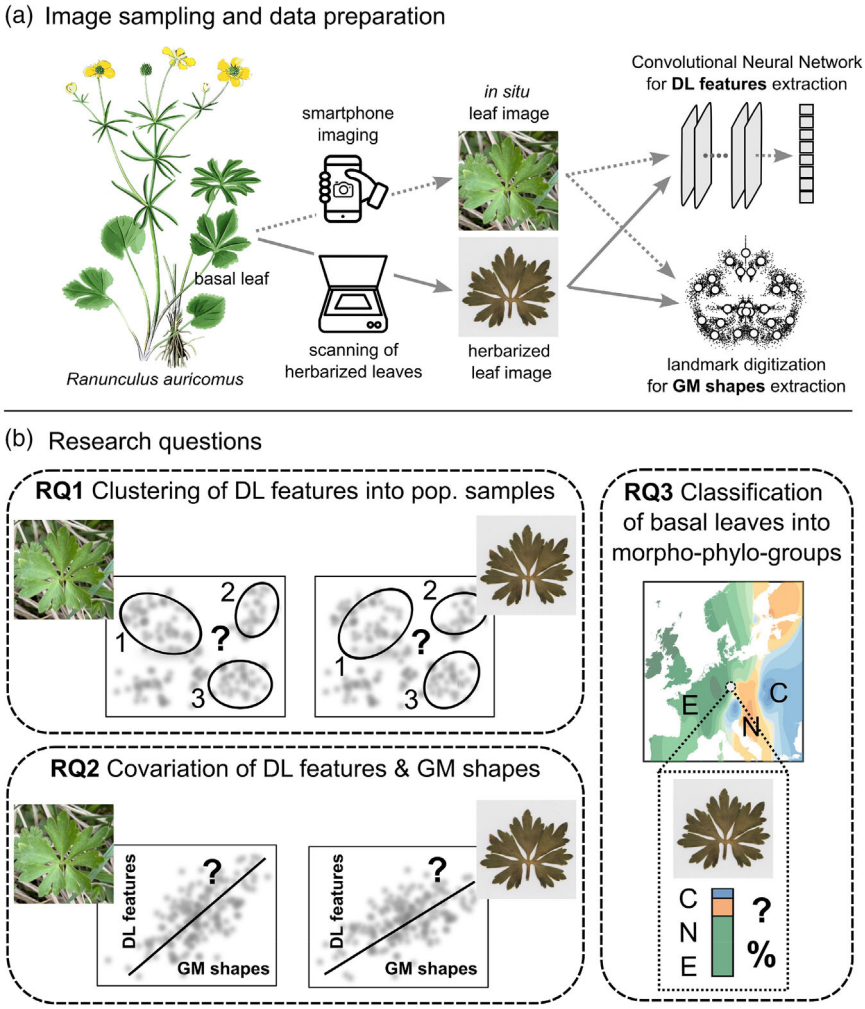

Figure 1. Workflow of this study from data acquisition to research questions.
(a) A flowering plant of *Ranunculus auricomus* with developed taxonomically informative basal leaves. Image data were acquired from identical leaves as smartphone images (= *in situ* leaf images) and by leaf scanning after herbarization (= herbarized leaf images). The *in situ* leaf images had a natural background, while the herbarized leaf images had a uniform background. From both *in situ* and herbarized images, we automatically extracted DL features (using a CNN) and manually extracted GM shapes (using a landmark digitization).
(b) Our research questions regarding clustering of DL features (RQ1), covariation of DL features and GM shapes (RQ2), and automatic classification of DL features into morpho-phylo-groups (RQ3).

the representation of leaf images by DL features (computer vision) with the representation of leaf shapes extracted as landmark configurations by GM, that is, GM shapes (biological vision). The statistical evaluation of computer vision by shape analysis (Figure S1) serves as an XAI approach to address three research questions (Figure 1b): (RQ1) Can we automatically and consistently cluster leaves into population samples using DL features extracted from identical leaves photographed *in situ* and after herbarization? (RQ2) Do the DL features extracted from leaf images contain information that reflect the biological shape of the photographed leaves? (RQ3) Can DL features provide a fine-grained taxonomic classification of herbarized leaves into morpho-phylo-groups?

RESULTS

Clustering of DL features into source population samples

Unsupervised nonlinear clustering (UMAP) of the DL features from the *in situ* images revealed clearly delineated clusters corresponding to the six populations (Figure 2a). The first UMAP axis separated populations KK203 (gray dots) and LHM001 (green dots), while the second UMAP axis separated populations LK0001 (purple dots) and LHT001 (turquoise dots). In contrast, the UMAP ordination of the herbarized leaf images (Figure 2b) resulted in weakly defined clusters, except for population KK065B (red dots). Notably, the UMAP visualization highlighted clear differences between the *in situ* and herbarized leaf image

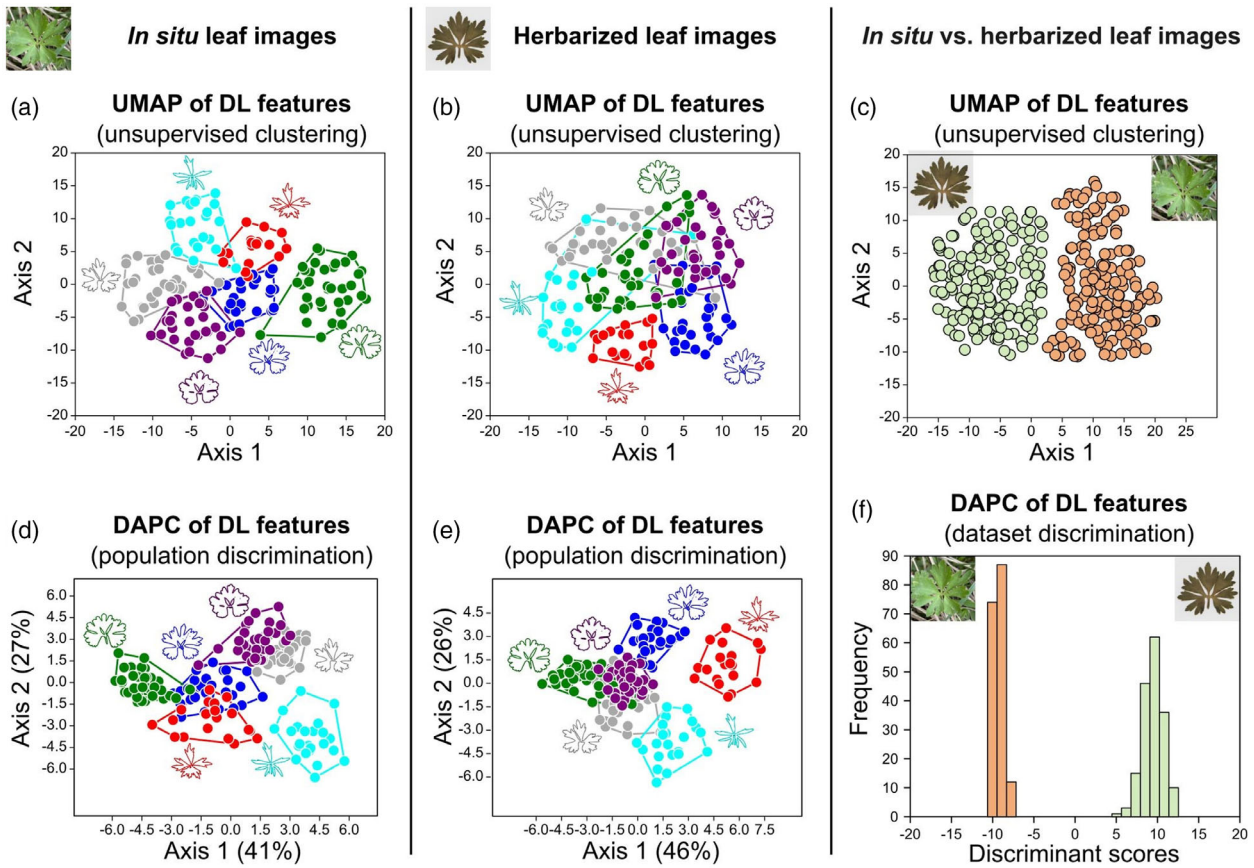

Figure 2. Clustering of DL features to infer differences between population samples.
(a, b) Nonlinear dimension reduction using UMAP for DL features extracted from *in situ* (a) and herbarized leaf images (b).
(c) The same method to highlight the difference between the *in situ* and corresponding herbarized leaf images.
(d, e) Linear dimension reduction with PCA followed by discriminant analysis (DAPC) to infer the statistical difference between the population samples of *in situ* (d) and herbarized leaf images (e).
(f) The DAPC to indicate the significant difference between the *in situ* and herbarized leaf image datasets. The six population samples are distinguished by color: blue = EH10333, red = KK065B, gray = KK203, dark green = LHM001, turquoise = LHT001, purple = LK0001.

datasets based on the extracted DL features (Figure 2c). Linear dimension reduction further confirmed that the *in situ* images, represented by their DL feature vectors, were not randomly scattered but clustered into separate groups based on their source populations (Figure 2d). Discriminant analysis (DAPC) of the six populations revealed statistically significant differences between them in both *in situ* ($P = 0.0010$) and herbarized leaf images ($P = 0.0010$). The two-dimensional ordination of the *in situ* images along the first two discriminant axes mirrored the unsupervised UMAP ordination, with well-separated populations such as LHM001 (green dots) and LHT001 (turquoise dots). Similarly, these populations remained distinct in the DAPC ordination of the herbarized leaf images (Figure 2e). The PERMANOVA test on the original (not reduced) feature vectors further supported significant differences between the six leaf image population samples, with Bonferroni-adjusted P values of 0.0060 for both the *in situ* and herbarized leaf image datasets. Additionally, DAPC indicated a significant difference ($P < 0.0001$) between the two image datasets themselves (Figure 2f).

Population differences inferred by DL features and GM shape analysis

Applying Grad-CAM to a CNN trained to discriminate between six populations of leaf images highlighted the regions of the basal leaf surface that corresponded to taxonomically relevant characters (Figure 3a). In some populations, for example, EH10333, the neural network primarily focused on the middle segment of the basal leaf (Figure 3a, upper part), consistent across both *in situ* and herbarized leaf images. In other populations, for example, KK065B, the attention of the neural network was distributed across various regions of the leaf surface (Figure 3a, lower part) and differed between *in situ* and herbarized leaf images. The Grad-CAM analysis revealed that the taxonomically important middle segment of the basal leaf (Figure 3b) often received the neural network's attention in

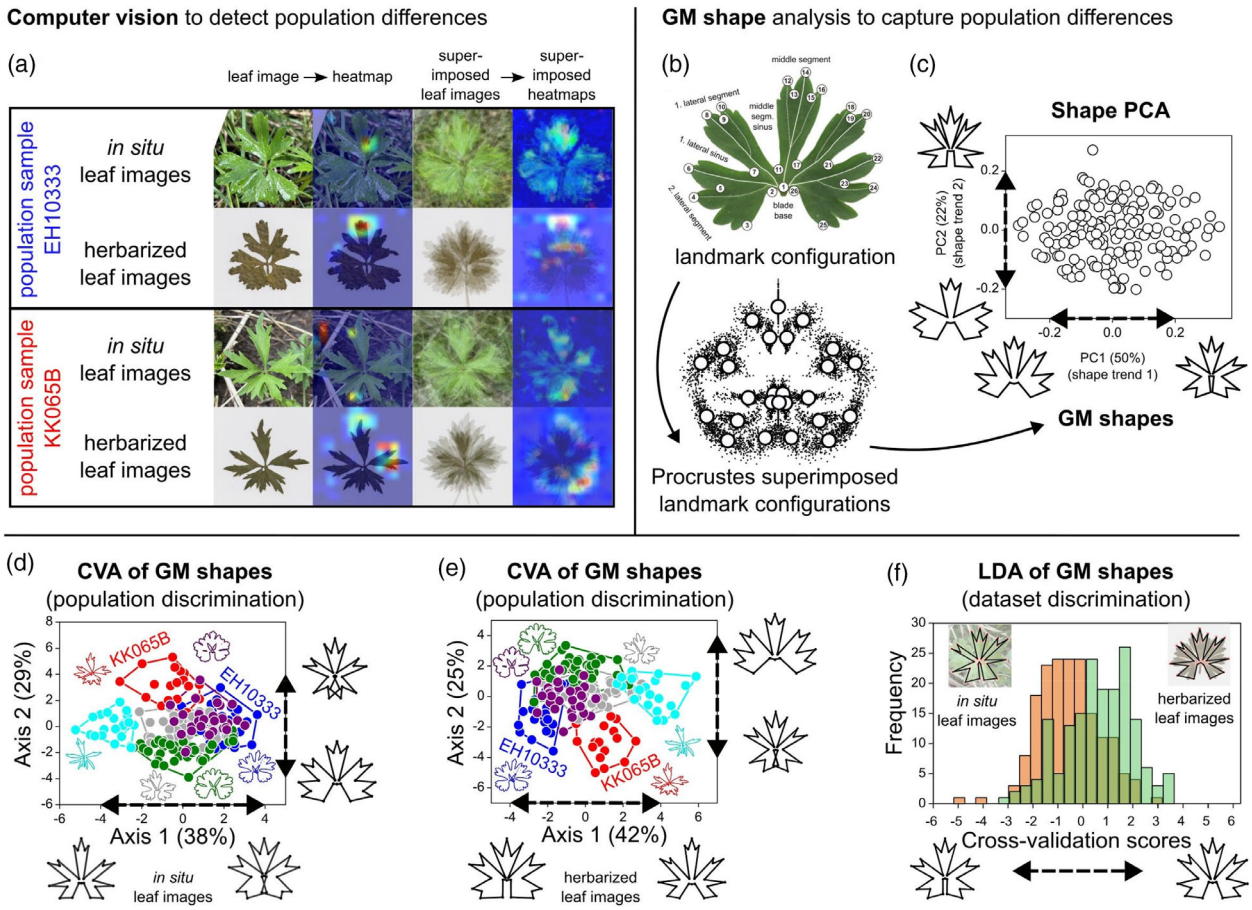

Figure 3. Computer vision versus geometric morphometric shape analysis to infer differences between population samples.
(a) Grad-CAM to illustrate the differences in the attention of a neural network when discriminating the population samples EH10333 (two top rows) and KK065B (two bottom rows). A representative heatmap and an average of six different heatmaps are shown for both population samples.
(b) Characteristic morphology of the taxonomically informative basal leaf of *Ranunculus auricomus* (Hodac et al., 2023). The 26 landmarks on the leaf outline are biologically homologous points—a basis for leaf shape extraction.
(c–e) (b) Procrustes-aligned (superimposed) landmark configurations (only the symmetric component is shown here) as a basis for extraction of shape variables by the PCA (c) and discrimination of population samples by canonical variates analysis (CVA) (d, e). Population samples EH10333 (red dots) and KK065B (blue dots) are highlighted, and the wireframe plots illustrate the GM shape trend that best separates the populations. Black arrows parallel to the canonical variate axes indicate the direction of leaf shape change that best separates the groups. Orange wireframe plots represent *in situ* leaf shapes and green wireframe plots represent herbarized leaf shapes.
(f) Discriminant analysis of GM shapes to infer the difference between *in situ* leaf images (orange) and corresponding herbarized leaf images (green).

both herbarized and *in situ* leaf images, often in combination with other regions of the basal leaf surface and outline, for example, the lateral segments.

GM shape analysis, based on the alignment of landmark configurations (Procrustes superimposition; Figure 3b), extracted leaf shape variation from the entire image dataset. The resulting shape PCA (Figure 3c; only the herbarized leaf image dataset is shown) visualized the leaf shapes within the morphospace, with the first principal component (PC1) explaining 50% of the leaf variation, mainly related to the shape of the leaf blade base. The second most important shape trend (PC2; 22%) of the leaf morphospace was related to the shape and orientation of the lateral segments. Linear discriminant analysis (CVA) of leaf shapes revealed significant shape differences among the six populations in both the *in situ* (Figure 3d) and herbarized (Figure 3e) leaf image datasets. CVA analysis further revealed significant shape differences (expressed as Procrustes distances) between all pairs of populations with all permutations $P < 0.0500$, within both the *in situ* and herbarized leaf image datasets. A small but significant difference was also found between the two image datasets (Figure 3f), with permutation $P < 0.0001$. This difference appeared in the leaf base, which was narrower in the *in situ* leaf images and broader in the herbarized leaf images.

Association of DL features and GM shapes

The decomposition of leaf shape variation into major shape trends using GM allowed further association of GM shape and DL features via correlation and covariation

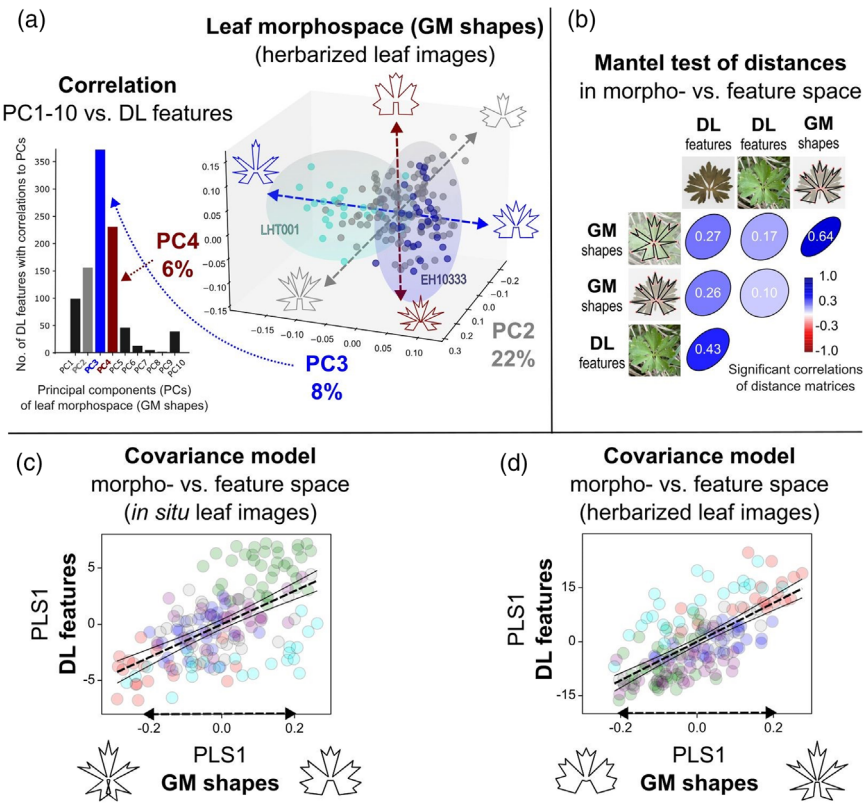

Figure 4. Leaf shape variation captured by deep learning and geometric morphometrics: association analyses.
(a) Scatterplot representing leaf morphospace (inferred from herbarized leaf images) showing leaf shape variation along three principal components. Wireframe plots illustrate leaf shape variation described by the principal components. Confidence ellipsoids are shown for two population samples (LHT001/turquoise, EH10333/blue) to highlight their separation in the leaf morphospace. The bar chart indicates how many DL features show a significant correlation with each of the principal components.
(b) Mantel test of GM shape differences in morphospace (Procrustes distances) and DL feature differences feature space (Euclidean distances). Values are Spearman's rank correlation coefficients, only significant values are shown.
(c, d) Partial least squares (PLS) analysis of the covariation between GM shapes in morphospace and DL features in feature space to extract the main direction of GM shape variation captured by DL features. (c) PLS scatterplot of the *in situ* leaf image dataset. (d) PLS scatterplot of the herbarized leaf image dataset. Circles in the scatterplots are colored according to six population samples.

analyses. The nine most important shape principal components, capturing more than 1% of the total shape variation, accounted for 94% (*in situ* leaf images) and 95% (herbarized leaf images) of the overall leaf shape variation. These shape PCs were significantly correlated ($r > 0.30$; $P < 0.0500$) with 786 DL features in the herbarized leaf images and 630 DL features in the *in situ* leaf images, among a total of 1792 DL features extracted per image. The third principal component (PC3) of the leaf morphospace accounted for the largest number of significant correlations with DL features (Figure 4a). Within the herbarized leaf images, 372 DL features were significantly correlated with PC3 (and 301 DL features in the *in situ* leaf images). The morphological trend most correlated with DL features described a change in leaf shape from leaves with shorter, wider, and more dissected middle segments to leaves with longer, thinner, and less dissected middle segments (blue leaf silhouettes/wireframe plots in Figure 4a). This observation, inferred from the herbarized leaf images, also applied to the *in situ* leaf images (figure not shown), where PC3 similarly accounted for most of the correlations with DL features. Among the nine most important principal components of the leaf morphospace, 20% of all DL features were consistently correlated with the principal components in both the herbarized and *in situ* leaf images.

Mantel correlation tests were applied to investigate whether leaf shape distances in morphospace corresponded to their distances in DL feature space, essentially testing if the neural network captured differences between leaf images in a way that was quantitatively comparable to differences in leaf shape alone. Within both the *in situ* and herbarized leaf image datasets, significant correlations were found between leaf differences in morphospace and DL feature space (Figure 4b). The correlation was slightly stronger within the herbarized leaf images ($r = 0.26$, $P = 0.0010$) compared to the *in situ* leaf images ($r = 0.17$, $P = 0.0010$). Significant correlations were also found between leaf scores on the discriminant axes in the

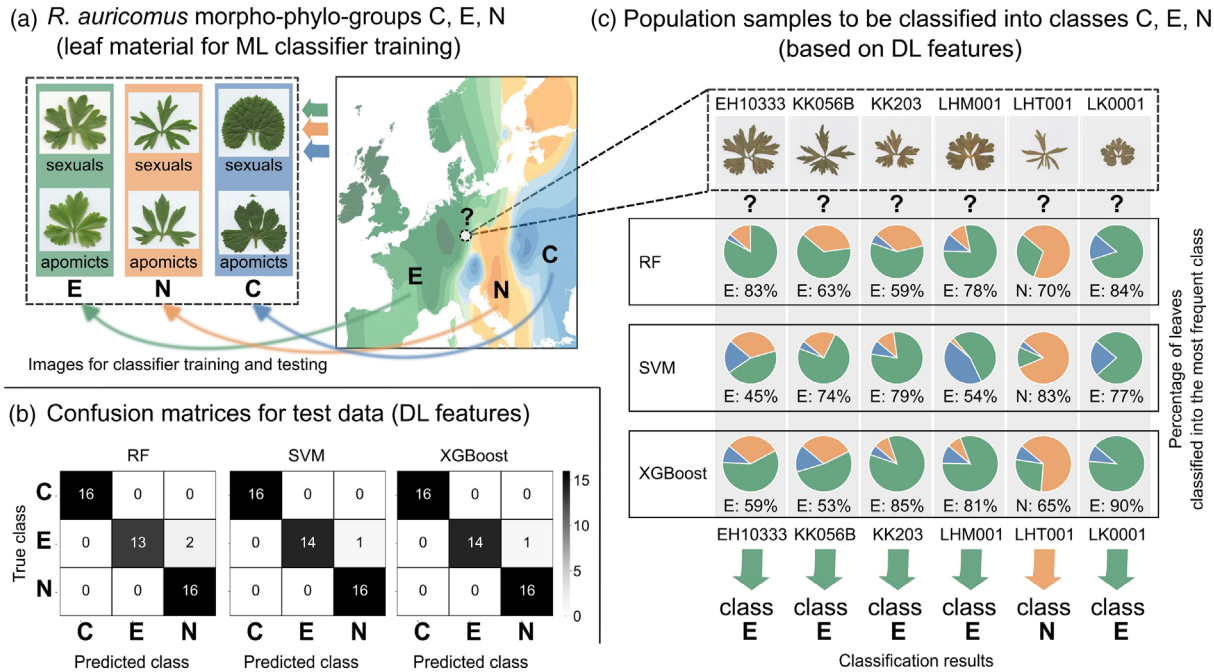

Figure 5. Automatic classification of herbarized leaf images based on DL features. The leaf images were classified into morpho-phylo-groups of the *Ranunculus auricomus* species complex, as derived from Karbstein et al. (2022).
(a) Examples of the training data—leaf images showing characteristic morphotypes of the three morpho-phylo-groups C (blue), E (green), and N (orange). Within the training dataset, each morpho-phylo-group group consists of leaf morphotypes representing both sexual and apomictic populations. The map shows the geographical distribution of the three morpho-phylo-groups in Europe.
(b) Confusion matrices to infer the classification accuracy achieved by different machine learning classification algorithms (RF, random forest; SVM, support vector machine; XGBoost, eXtreme gradient boosting) after training and classification of test data.
(c) Automatic classification of the six population samples after training the classifiers on leaf images representing the three morpho-phylo-groups C, E, N. The herbarized leaf images show the characteristic leaf morphotype for each population sample, and the pie charts illustrate the proportions of leaves within each population sample classified into one to three classes. The final classification of the population samples resulted from the most frequent class as consistently classified by the three different classifiers.

morpho and DL feature spaces. The vector that best separated populations in the DL feature space was significantly correlated ($r = 0.54$; $P < 0.0500$) with a GM shape change describing variation at the blade base (Figure S2a–c). The general covariation model of GM shape and DL feature association (computed via PLS analysis) indicated a stronger association in the herbarized leaf images ($R = 0.68$, $P = 0.0001$) than in the *in situ* leaf images ($R = 0.58$, $P = 0.0001$). Within both image datasets, the covariation model showed that the variation in DL features is mostly associated with the shape variation focused on the blade base and the dissections of the lateral segments. A closer look at the particular features associated with different leaf shape trends revealed that different leaf shape changes were associated with different sets of DL features (Figure S3a,b).

Classification of leaves within the *R. auricomus* species complex using DL features and GM shapes

The DL features extracted from images of sexual and apomictic leaf morphotypes (Figure 5a), in combination with the three selected classification algorithms, provided high accuracies for both the validation data partition and the unseen test data (Figure 5b). Random forest achieved a classification accuracy of 0.97 for both validation and test data. Support vector machine achieved a classification accuracy of 0.97 for validation data and 0.98 for test data. XGBoost achieved a classification accuracy of 0.97 for validation data and 0.98 for test data. Automatic classification of the Thuringian population samples based on DL features (Figure 5c) therefore yielded consistent results for the three machine learning classifiers. Based on the leaf images, five of the six Thuringian populations could be classified into morpho-phylo-group E (Figure 5c), referring to the sexual progenitor species *Ranunculus envalirensis*. One population sample (LHT001) was consistently classified in morpho-phylo-group N, referring to the sexual progenitor *R. notabilis*. For the GM shape data, the validation and test accuracies were lower than for DL features described above. RF achieved a validation accuracy of 0.72, and test accuracy of 0.71, SVM achieved a validation accuracy of 0.73, and test accuracy of 0.60, XGBoost achieved a validation accuracy of 0.73, and test accuracy of 0.67. Nevertheless, the classification of the six population samples

from Thuringia resulted in class assignments consistent with the DL feature data (Figure S4).

DISCUSSION

The present study shows that DL captures the shape of morphological traits, whether in smartphone images taken in the field or in standardized images of herbarium specimens. Our approach to XAI—a combination of DL and statistical shape analysis—offers novel insights into the automatic recognition of biological shapes from images. Our work is innovative in two ways: (1) we analyzed for the first time DL features extracted from identical leaves imaged *in situ* and after herbarization and (2) we provided statistical support for leaf shape being encoded in DL features automatically extracted from leaf images.

DL captured even subtle differences between populations

Previous computer vision studies have not compared images of the same leaves taken *in situ* and after herbarization. Surprisingly, despite a comparatively uniform background, herbarized leaf images showed greater variation in DL features than *in situ* images. This aligns with the observation from benchmark datasets (PlantCLEF 2020 and 2021) that images of herbarized leaves may be preferable for capturing plant morphology (Chulif et al., 2023). However, *in situ* leaf images captured background noise and illumination variations, which can influence what a DL model learns, as also shown in our Grad-CAM experiments (Figure 3a), where sometimes image attributes other than leaf shape were also learned. This is consistent with previous conclusions that CNN-based classification is sensitive to image background, especially for small image datasets (Barbedo, 2018). Our Grad-CAM analysis showed differences in neural network attention when discriminating between population samples of *in situ* and herbarized leaf images. In addition to the explanation regarding different backgrounds, also leaf morphology itself can undergo significant changes during the drying process (Blonder et al., 2012; Carranza-Rojas et al., 2017; Tomaszewski & Górzkowska, 2016). Our GM analysis revealed that the primary difference in leaf shape between *in situ* and herbarium images was due to the treatment of the leaf material. The fresh *in situ* leaves and pressed herbarium leaves exhibited a slightly different shape in the basal part. Nonetheless, the geometric morphometric approach captured similar overall leaf shapes from both *in situ* and herbarium images. Although the morphology of herbarized plants may not always be directly interchangeable with that of fresh material, their inclusion greatly expands the databases of preserved morphological characters (e.g., GBIF) and plays an important role in plant taxonomy (Wu et al., 2023). Unsupervised UMAP clustering of DL features successfully distinguished all population samples as separate clusters, supporting the applicability of DL features in discriminating classes above the species level, as previously demonstrated, for example, for Nile tilapia fish ecotypes (Wöber et al., 2021). In our case, DL features also discriminated between *in situ* and herbarium specimens more effectively than GM shapes, irrespective of whether the background was natural or plain. This is likely because DL features captured more complex leaf shape characteristics that the simpler GM shape approach can achieve to distinguish between populations.

Deep learning automatically recognized leaf shapes from images

Handmade morphological features and GM with expert input provide biological interpretability where homologous and analogous biological structures need to be quantified (de Lima et al., 2024). Phenotypic plasticity, the ability of a genotype to produce different phenotypes in response to environmental differences, generates complexity in morphology (Bucksch et al., 2017) that requires biologically interpretable analytical approaches to separate technical bias from genetic and environmental factors. Besides genetic background, bioclimatic parameters or altitude can also influence leaf phenotypes in nature, as shown, for example, for *R. auricomus* basal leaves (Hodac et al., 2023). Our analyses showed that a stronger association of DL features with biological shapes was observed in herbarized leaf images than in *in situ* leaf images. Furthermore, different sets of DL features were correlated with biological shape variation in herbarized and *in situ* leaf images. Comparable studies on the direct biological interpretability of DL features are scarce. A concept of *mones* as abstract morphological genes derived from DL features has been applied in digital pathology (Foroughipour et al., 2022). Our XAI approach searches for associations between DL features and taxonomically relevant shapes captured by GM. Unlike traditional statistical shape modeling (Laga et al., 2013, 2014; Woods et al., 2017), GM focuses on those regions of biological objects that are important to taxonomists or evolutionary biologists. In traditional taxonomic approaches, and presumably in DL, shape is the most discriminating feature of plant leaves (Karbstein et al., 2020; Stuessy, 2009; Wäldchen & Mäder, 2018). In our XAI workflow, we manually digitized leaf morphometric shapes from the preprocessed smartphone images, and the biological interpretability of our custom landmark set is based on previous evolutionary and ecological studies on the *R. auricomus* model system (Hodac et al., 2023; Karbstein et al., 2022). Manual landmark digitization is a common approach in plant morphometric studies (Savriama, 2018; Stojnić et al., 2022; Viscosi & Cardini, 2011), and can be accomplished using a variety of free software, such as geomorph (Baken et al., 2021), TpsDig2 (Rohlf, 2015), or ImageJ (Rueden et al., 2017). However, landmark placement (digitization) might be automated in the future using a variety of approaches, including machine learning classifiers (Porto &

Voje, 2020), feedforward neural networks (Devine et al., 2020), CNN architectures (Nguyen et al., 2022; Rodrigues et al., 2022; Shuai et al., 2023; Yun et al., 2022), CNN with transformer (Song et al., 2024), Spatial Transformer Generative Adversarial Network (Wang et al., 2022), LSTM-RNN (Chen et al., 2017), or point cloud-based approaches (Porto et al., 2021).

Despite the widespread use of Grad-CAM to better understand automatic classification of biological objects, few studies have compared how CNN features relate to morphological characters relevant to taxonomy. One of the few comparable studies examined the shape of mussels (Kiel, 2021) and showed that focal areas of a CNN aligned with morphological characters used by taxonomists. Another study comparing morphological identifications by citizen scientists with CNN-based classification of lizards demonstrated the superior accuracy of computer vision in recognizing cryptic species (Pinho et al., 2023). Grad-CAM has also been utilized in entomology to show how CNN classifications agree with biologically meaningful morphological features in the automatic identification of mosquitoes (Adhane et al., 2021) or midges (Milošević et al., 2020). Our experiments with Grad-CAM revealed that the neural networks distributed their attention across multiple regions of the leaf surface rather than consistently focusing on a single most important area, although there was an observable tendency to frequently focus on the central segment of basal leaves in *R. auricomus* (Figure 3a), a morphological trait critical to the taxonomy of our specific model plant group (Borchers-Kolb, 1983; Hörandl & Gutermann, 1995). The covariation models also showed that the DL features extracted from the leaf images were significantly associated with differences in leaf shape, especially with the taxonomically relevant variations in the leaf middle segment or basal sinus.

DL features for classification of evolutionarily intricate species complexes

We investigated whether DL features extracted for morphologically distinct population samples allow automatic classification into morpho-phylo-groups within the *R. auricomus* species complex (Hodac et al., 2023; Karbstein et al., 2022). Previous studies have already shown that training on herbarized leaf images from one region can be transferred to herbarized leaf images from another region (Carranza-Rojas et al., 2017). Our study followed a similar approach, where we trained the classifiers on leaf images from different regions of Europe in order to test the classifier on images from Central Europe. Based on the majority rule, five Thurigian population samples were assigned to the morpho-phylo-group E and one to the morpho-phylo-group N. It is noteworthy that within a population sample, leaves were often classified in up to three different classes. This could be due to the high morphological variation within each population, which exceeds the morphological limits of the morpho-phylo-group. Furthermore, the possibility of genetic hybrids of three subgenomes, as previously reported for three of the six asexual populations (Karbstein et al., 2022), with dominance of subgenome E and smaller proportions of subgenomes N and C, likely contributes to this variation. In addition, the classification of the herbarized leaf images might be biased due to the use of DL features extracted with a neural network trained on fresh plant images. To overcome such bias in the future, a herbarium-field triplet loss network architecture has been proposed that addresses transfer learning between herbarium and field data (Chulif et al., 2023). For our model plant group, classification accuracy was higher when using DL features compared to geometric morphometric (GM) shapes. DL features likely capture a more complex representation of leaf morphology, including subtle variations in shape, texture, and patterns that a simplified GM-based shape representation misses. Additionally, DL feature extraction is automated and data-driven, whereas GM landmarks require manual selection of biologically homologous points, which are unlikely to capture the full complexity of leaf shapes. However, despite the lower classification accuracies achieved by the GM approach, the final classification results (assignments into the morpho-phylo-groups) were almost identical for both GM shapes and DL features. This suggests that both methods are capable of recognizing concordant patterns of overall class discrimination.

Perspectives on smartphone phenotyping

We propose an efficient and easy-to-use approach to plant phenotyping using a novel method of explainable AI (XAI). Our approach captures and classifies leaf morphotypes and reveals which DL features account for the variation in biological shape. Samples of target morphological traits (e.g., leaves, flowers, stems, etc.) can be easily imaged *in situ* using smartphone apps, with observations registered using a custom protocol provided by the app, essentially functioning as a digital herbarium (Boho et al., 2020). Our approach differs from related studies that have employed smartphones alongside additional equipment, such as for medicinal plant phenotyping (Azadnia & Kheiralipour, 2021) or black tea quality grading (Li et al., 2021). Instead, our method aligns more closely with citizen science initiatives that utilize smartphone imaging, which relies on handheld image capture without the need for additional costly equipment, as already employed in maize phenotyping (Liu et al., 2021; Müller-Linow et al., 2019) or tobacco leaf maturity analysis (Sun et al., 2023). To further speed up the phenotyping process, the automated detection of relevant morphological structures from raw smartphone images can be done automatically, for example, by using a U-Net architecture for plant structure segmentation (Yang et al., 2020) or the GinJinn2 DL toolbox (Ott &

Lautenschlager, 2022). Leveraging leaf segmentation, automated landmark digitization followed by Procrustes normalization can help align leaf shapes from differently rotated images. Combining the strengths of GM and DL methods could benefit from reproducible shape matching, thereby enhancing the classification model's performance. Automated processing of smartphone-captured morphological traits reveals valuable data about species in their natural environment, as these data contribute to growing web databases of citizen science images (e.g., iNaturalist, GBIF). Large collections of plant trait images have already enabled machine learning-based automatic classification of petal pigmentation (Perez-Udell et al., 2023), and flower colors sampled with an R shiny pipeline have been used to study non-random spatial patterns in flower color distribution in American wallflowers (Luong et al., 2023). The use of smartphones to collect plant phenotypic data in natural environments is a promising area for integrative taxonomy based on machine learning, where genomic data can be efficiently supported by informative morphological data (Karbstein et al., 2024). The use of low-cost, low-threshold smartphone imaging, hand in hand with machine learning and citizen science, could advance efforts toward global plant conservation initiatives (Corlett, 2023).

EXPERIMENTAL PROCEDURES

Sampling and image preprocessing

We assembled six population samples of basal leaf images (Figure 1a) representing different morphotypes within the *R. auricomus* species complex. These six populations (all sampled in central Germany, Thuringia; Table S1) were likely clonal/apomictic, exhibiting reduced flowers and growing outside the restricted range of all known sexual progenitors within the *R. auricomus* species complex (Karbstein et al., 2020, 2021). The sampled populations originated from the biogeographic range where the morpho-phylo-group E (a group of clonal morphospecies with a major subgenome contribution from the sexual progenitor species *R. envalirensis*) has a high prevalence (Karbstein et al., 2022). Morpho-phylo-group E is mainly distinguished by basal and stem leaf morphology and genomic features from the co-occurring European groups N, named after the sexual progenitor species *R. notabilis*, and C, named after the sexual progenitor species *R. cassubicifolius* (Karbstein et al., 2020). The six populations sampled in central Germany exhibited morphological variation in basal leaf shape, the key taxonomic character in this species complex (Hörandl & Gutermann, 1995; Melzheimer & Hörandl, 2022). These basal leaves provide a set of geometric morphometric landmarks already used for integrative systematics and evolutionary studies of this group (Hodac et al., 2023; Karbstein et al., 2020).

To capture the morphological variation within each population (sampling site), taxonomically informative basal leaves from 20 flowering-stage plants were imaged (Figure 1a). For each individual plant, the two most dissected basal leaves were photographed from the adaxial view (Rzanny et al., 2019) and then collected for herbarium preparation. Leaf images were captured directly *in situ* using the smartphone application Flora Capture (Boho et al., 2020), which allows systematic recording of individuals while storing metadata such as GPS coordinates. Herbarized leaves were scanned from the adaxial view using a Canon LiDE 400 scanner and labeled identically to their *in situ* counterparts. To minimize potential artificial differences (e.g., leaf position and orientation) between the *in situ* and herbarized leaf image datasets, all leaves were rotated to achieve similar orientation. This was necessary because we analyzed the leaves using both GM and a CNN in parallel, and GM requires that objects have a similar rotation. Also, the images we used to train the machine learning classifiers by Hodac et al. (2023) used identical image treatment, that is, rotating all images to achieve similar leaf orientation. The herbarized leaf images were manually cropped to a standard size of 800 × 800 pixels, preserving the original leaf size information, and the *in situ* leaf images were manually cropped to a fixed 1:1 width to height ratio. Preprocessing was done using the GIMP 2.10 image editor. The final sample size was 346 leaf images, and the number of images per population sample is given in Table S1. In the present study, we intentionally focused on using images with natural backgrounds to reflect the conditions under which DL models would typically be applied in real-world scenarios, such as *in situ* imaging and automatic identification of plant organs. Although segmenting leaves from their background could potentially enhance the performance of DL classification models, this approach involves a significantly greater effort (Rzanny et al., 2017). Therefore, the aim of this study was to evaluate whether DL methods applied to raw, unprocessed images can effectively capture differences in leaf shape compared to GM, without the labor-intensive step of spatial segmentation.

Extraction of DL features and dimension reduction

The research questions addressed in this study are illustrated in Figure 1(b). To assess whether DL features extracted from leaf images using FloraNet, a neural network trained on more than 16 000 plant species (Mäder et al., 2021), allow clustering of the images according to their source population samples, their dimensionality was reduced using a nonlinear technique called uniform manifold approximation and projection (UMAP; parameters provided in Methods S1). UMAP is a powerful method capable of handling the nonlinear relationships often present in high-dimensional data (McInnes et al., 2018). To support the robustness of the DL feature clustering with a linear dimension reduction method, principal component analysis (PCA) was also performed on the same data (Jolliffe, 2002). The scores of the leaf representations (DL features) in the lower dimensional space obtained from PCA were then used to test for significant differences between pairs of populations. This was achieved using a linear discriminant analysis of principal components, DAPC (Jombart et al., 2010). A two-group discriminant analysis was then performed to compare the *in situ* and herbarized leaf image datasets. The DAPC analysis was implemented using the adegenet package (Jombart, 2008) in R (R Core Team, 2022). Differences between groups in the reduced space were further tested using ANalysis Of SIMilarity (ANOSIM), implemented in the R package vegan (Dixon, 2003). As an alternative test for population differences based on the original DL feature vectors, a permutational multivariate analysis of variance/PERMANOVA (Anderson, 2017) with a post hoc test (using Bonferroni-corrected p-values) was performed in the scikit-bio python library (Pedregosa et al., 2011).

Grad-CAM to visualize population differences

To gain insight into how the neural network discriminates between population samples, we applied Grad-CAM. This technique highlights the image regions crucial for the network to predict a specific class (Selvaraju et al., 2020). In our case, we had six

classes corresponding to six population samples of leaf images. The output of Grad-CAM (details provided in Methods S2) was visualized as heatmaps overlaid onto the original images. We used TensorFlow (Abadi et al., 2016) with the Keras API to operate the underlying neural network model. Matplotlib (Hunter, 2007) was used to visualize the images with overlaid Grad-CAM heatmaps. Finally, the images and their heatmaps were averaged over the population samples using NumPy (Harris et al., 2020).

Geometric morphometrics to evaluate leaf shape variation

GM allows the extraction of biological shapes from images. In this study, we followed the methodology previously established for the basal leaves of *R. auricomus* (Hodac et al., 2023; Karbstein et al., 2020). The leaf shapes captured in the images were digitized by 26 manually placed 2D landmarks using the program TpsDig2 version 2.32 (Rohlf, 2015). Landmark configurations were subjected to Procrustes superposition (Zelditch et al., 2012) to separate shape and non-shape information and to separate symmetric and asymmetric components of leaf shape variation. Procrustes superimposition and subsequent morphometric analyses were performed in the comprehensive morphometric software MorphoJ version 1.07a (Klingenberg, 2011). Only the symmetric component of shape variation was used to obtain shape variables. Differences in leaf shape between population samples were inferred using canonical variates analysis (CVA), a linear discriminant analysis widely used in shape studies (Caiza Guamba et al., 2021; Nery & Fiaschi, 2019; Yee et al., 2011), and tested with permutation tests (10 000 permutations). Morphological distances between particular leaf shapes were inferred as Procrustes distances computed in the program TpsSmall version 1.20 (Rohlf, 2015).

Association of DL features and GM shapes

To analyze the key shape variations within the leaf morphospace, we used shape PCA. To link these shape trends to the DL features, we extracted the leaf shape scores on the principal components and correlated them with the corresponding DL features using Spearman's rankorder correlation coefficient in scipy.stats (Virtanen et al., 2020). This analysis revealed which morphological trends within the leaf morphospace were most likely to be captured by the DL features. In addition, we sought to determine what proportion of the DL features describing a leaf image were associated with the leaf shape itself. Furthermore, we investigated whether the object (leaf image) distances inferred from the DL features were consistent with those captured by GM based on leaf shape. To gain deeper insight into the pairwise differences of leaf image representations in feature space, we computed a Euclidean distance matrix. We then compared the distances of the leaf representations in feature space with their distances in leaf morphospace, expressed as Procrustes distances. Correlations between these distance matrices were computed using the Mantel test in PAST version 4.15 (Hammer et al., 2001). The significance of the correlation coefficient was assessed using a permutation test (10 000 permutations). Similarly, we compared the ordination of DL feature vectors in feature space and GM shapes in morphospace after maximizing the differences between population samples. The object scores (DL feature vectors or GM shapes) obtained from the discriminant analyses were then tested for association using Spearman's rank-order correlation coefficient. Finally, we examined the overall association between DL features and GM shapes using partial least squares (PLS) in MorphoJ version 1.07a (Klingenberg, 2011) to infer a comprehensive covariation model of leaf morphology captured by the DL features. These analyses were performed on both the *in situ* and herbarized leaf image datasets.

Machine learning based on DL features and GM shapes for automatic classification of leaf images

We investigated whether the DL features extracted from herbarized leaf images of the populations sampled in Thuringia could be used to automatically classify them into the morpho-phylo-groups E, C, or N recognized within the *R. auricomus* species complex. The basal leaf images used to train the machine learning classifiers were previously labeled (Hodac et al., 2023), stored online (Karbstein et al., 2023), and reassembled here to include leaf morphotypes representative of all three morpho-phylo-groups C, E, and N (Karbstein et al., 2022). The balanced training dataset consisted of 366 leaf images, divided into three classes corresponding to the three morpho-phylo-groups C, E, and N. Each class included leaf morphotypes from both sexual species and apomictic lineages (in an almost 1:1 ratio), revealed by scanning fresh leaves of cultivated plants (Hodac et al., 2023; Karbstein et al., 2020). The DL features were extracted from the leaf images in the same way as from the six Thuringian population samples using the FloraNet pipeline (Mäder et al., 2021). Three different classifier algorithms (random forest/RF, support vector machine/SVM, eXtreme gradient boosting/XGBoost) were applied using the machine learning library scikit-learn (Pedregosa et al., 2011). The performance of the classifiers was evaluated based on validation and test classification accuracy, with test data taken from the same source as the training data but belonging to a different subset. Identical classification experiments were also conducted using vectorized landmark configurations derived from the same leaf images as in the DL-based approach. Before entering the machine learning procedures, the vectorized landmark configurations were first Procrustes superimposed and symmetrized to match the landmark data preprocessing described earlier.

ACKNOWLEDGMENTS

We thank Negin Katal, Talie Musavi, and Alice Fritz for their support with sampling. This study was funded by the German Federal Ministry of Education and Research (BMBF) grant: 01IS20062, the German Federal Ministry for the Environment, Nature Conservation, Nuclear Safety and Consumer Protection (BMUV) grants: 3519685A08, 3519685B08 and 67KI2086, and the Thuringian Ministry for Environment, Energy and Nature Conservation grant: 0901-44-8652. Open Access funding enabled and organized by Projekt DEAL.

CONFLICT OF INTEREST

The authors declare no competing interests.

DATA AVAILABILITY STATEMENT

All new images have been deposited on Figshare (https://figshare.com/s/5eca8beee408f640b386). The codes are available from GitHub (https://github.com/lhodac2/Ranunculus_XAI_python_codes).

SUPPORTING INFORMATION

Additional Supporting Information may be found in the online version of this article.

Figure S1. An overview of the methods used.

Figure S2. Population differences inferred from DL features and GM shapes.

Figure S3. Partial least squares (PLS) analysis to infer the covariance between DL features and GM shapes.

Figure S4. Automatic classification of leaf images: a comparison of DL features and GM shapes.

Table S1. Six population samples of leaf images.

Methods S1. UMAP settings.

Methods S2. Grad-CAM settings.

REFERENCES

Abadi, M., **Barham, P.**, **Chen, J.**, **Chen, Z.**, **Davis, A.**, **Dean, J. *et al.*** (2016) TensorFlow: a system for large-scale machine learning. *arXiv:1605.08695 [cs.DC]*. Available from: https://doi.org/10.48550/arXiv.1605.08695

Adhane, G., **Dehshibi, M.M.** & **Masip, D.** (2021) A deep convolutional neural network for classification of *Aedes albopictus* mosquitoes. *IEEE Access*, **9**, 72681–72690. Available from: https://doi.org/10.1109/ACCESS.2021.3079700

Anderson, M.J. (2017) Permutational multivariate analysis of variance (PERMANOVA). In: *Wiley StatsRef: statistics reference online*. Hoboken: John Wiley & Sons, Ltd, pp. 1–15. Available from: https://doi.org/10.1002/9781118445112.stat07841

Azadnia, R. & **Kheiralipour, K.** (2021) Recognition of leaves of different medicinal plant species using a robust image processing algorithm and artificial neural networks classifier. *Journal of Applied Research on Medicinal and Aromatic Plants*, **25**, 100327. Available from: https://doi.org/10.1016/j.jarmap.2021.100327

Baken, E.K., **Collyer, M.L.**, **Kaliontzopoulou, A.** & **Adams, D.C.** (2021) Geomorph v4.0 and gmShiny: enhanced analytics and a new graphical interface for a comprehensive morphometric experience. *Methods in Ecology and Evolution*, **12**, 2355–2363. Available from: https://doi.org/10.1111/2041-210x.13723

Barbedo, J.G.A. (2018) Impact of dataset size and variety on the effectiveness of deep learning and transfer learning for plant disease classification. *Computers and Electronics in Agriculture*, **153**, 46–53. Available from: https://doi.org/10.1016/j.compag.2018.08.013

Beikmohammadi, A., **Faez, K.** & **Motallebi, A.** (2022) SWP-LeafNET: a novel multistage approach for plant leaf identification based on deep CNN. *Expert Systems with Applications*, **202**, 117470. Available from: https://doi.org/10.1016/j.eswa.2022.117470

Bellin, N., **Calzolari, M.**, **Magoga, G.**, **Callegari, E.**, **Bonilauri, P.**, **Lelli, D. *et al.*** (2022) Unsupervised machine learning and geometric morphometrics as tools for the identification of inter and intraspecific variations in the *Anopheles maculipennis* complex. *Acta Tropica*, **233**, 106585. Available from: https://doi.org/10.1016/j.actatropica.2022.106585

Blonder, B., **Buzzard, V.**, **Simova, I.**, **Sloat, L.**, **Boyle, B.**, **Lipson, R. *et al.*** (2012) The leaf-area shrinkage effect can bias paleoclimate and ecology research. *American Journal of Botany*, **99**(11), 1756–1763. Available from: https://doi.org/10.3732/ajb.1200062

Boho, D., **Rzanny, M.**, **Wäldchen, J.**, **Nitsche, F.**, **Deggelmann, A.**, **Wittich, H.C. *et al.*** (2020) Flora capture: a citizen science application for collecting structured plant observations. *BMC Bioinformatics*, **21**(1), 576. Available from: https://doi.org/10.1186/s12859-020-03920-9

Bonhomme, V., **Bouby, L.**, **Claude, J.**, **Dham, C.**, **Gros-Balthazard, M.**, **Ivorra, S. *et al.*** (2023) Deep learning versus geometric morphometrics for archaeobotanical domestication study and subspecific identification. *bioRxiv*. Available from: https://doi.org/10.1101/2023.09.15.557939

Bookstein, F.L. (1997) *Morphometric tools for landmark data*. Cambridge: Cambridge University Press.

Borchers-Kolb, E. (1983) Ranunculus sect. Auricomus in Bayern und den angrenzenden Gebieten. II. Spezieller Teil. *Mitteilungen der Botanischen Staatssammlung München*, **19**, 363–429.

Borowiec, M.L., **Dikow, R.B.**, **Frandsen, P.B.**, **McKeeken, A.**, **Valentini, G.** & **White, A.E.** (2022) Deep learning as a tool for ecology and evolution. *Methods in Ecology and Evolution*, **13**(8), 1640–1660. Available from: https://doi.org/10.1111/2041-210X.13901

Borraz-Martínez, S., **Simó, J.**, **Gras, A.**, **Mestre, M.**, **Boqué, R.** & **Tarrés, F.** (2022) Combining computer vision and deep learning to classify varieties of *Prunus dulcis* for the nursery plant industry. *Journal of Chemometrics*, **36**(2), e3388. Available from: https://doi.org/10.1002/cem.3388

Bucksch, A., **Atta-Boateng, A.**, **Azihou, A.F.**, **Battogtokh, D.**, **Baumgartner, A.**, **Binder, B.M. *et al.*** (2017) Morphological plant modeling: unleashing geometric and topological potential within the plant sciences. *Frontiers in Plant Science*, **8**, 900. Available from: https://doi.org/10.3389/fpls.2017.00900

Caiza Guamba, J.C., **Corredor, D.**, **Galárraga, C.**, **Herdoiza, J.P.**, **Santillán, M.** & **Segovia-Salcedo, M.C.** (2021) Geometry morphometrics of plant structures as a phenotypic tool to differentiate *Polylepis incana* Kunth. and *Polylepis racemosa* Ruiz & Pav. reforested jointly in Ecuador. *Neotropical Biodiversity*, **7**(1), 121–134. Available from: https://doi.org/10.1080/23766808.2021.1906138

Carranza-Rojas, J., **Goeau, H.**, **Bonnet, P.**, **Mata-Montero, E.** & **Joly, A.** (2017) Going deeper in the automated identification of herbarium specimens. *BMC Evolutionary Biology*, **17**(1), 181. Available from: https://doi.org/10.1186/s12862-017-1014-z

Chen, Y., **Yang, J.** & **Qian, J.** (2017) Recurrent neural network for facial landmark detection. *Neurocomputing*, **219**, 26–38. Available from: https://doi.org/10.1016/j.neucom.2016.09.015

Chulif, S., **Lee, S.H.**, **Chang, Y.L.** & **Chai, K.C.** (2023) A machine learning approach for cross-domain plant identification using herbarium specimens. *Neural Computing and Applications*, **35**(8), 5963–5985. Available from: https://doi.org/10.1007/s00521-022-07951-6

Corlett, R.T. (2023) Achieving zero extinction for land plants. *Trends in Plant Science*, **28**(8), 913–923. Available from: https://doi.org/10.1016/j.tplants.2023.03.019

de Benito Fernández, M., **Martínez, D.L.**, **González-Briones, A.**, **Chamoso, P.** & **Corchado, E.S.** (2023) Evaluation of XAI models for interpretation of deep learning techniques' results in automated plant disease diagnosis. In: *Trends in sustainable smart cities and territories*. Cham: Springer, pp. 417–428. Available from: https://doi.org/10.1007/978-3-03136957-536

de Lima, V.R., **de Morais, M.C.C.** & **Kirchgatter, K.** (2024) Integrating artificial intelligence and wing geometric morphometry to automate mosquito classification. *Acta Tropica*, **249**, 107089. Available from: https://doi.org/10.1016/j.actatropica.2023.107089

Devine, J., **Aponte, J.D.**, **Katz, D.C.**, **Liu, W.**, **Vercio, L.D.L.**, **Forkert, N.D. *et al.*** (2020) A registration and deep learning approach to automated landmark detection for geometric morphometrics. *Evolutionary Biology*, **47**(3), 246–259. Available from: https://doi.org/10.1007/s11692-020-09508-8

Dixon, P. (2003) VEGAN, a package of R functions for community ecology. *Journal of Vegetation Science*, **14**(6), 927–930. Available from: https://doi.org/10.1111/j.1654-1103.2003.tb02228.x

Foroughipour, A., **White, B.S.**, **Park, J.**, **Sheridan, T.B.** & **Chuang, J.H.** (2022) Deep learning features encode interpretable morphologies within histological images. *Scientific Reports*, **12**, 9428. Available from: https://doi.org/10.1038/s41598-022-13541-2

Gunning, D. & **Aha, D.** (2019) DARPA's explainable artificial intelligence (XAI) program. *AI Magazine*, **40**(2), 44–58. Available from: https://doi.org/10.1609/aimag.v40i2.2850

Hammer, O., **Harper, D.** & **Ryan, P.** (2001) PAST: paleontological statistics software package for education and data analysis. *Palaeontologia Electronica*, **4**, 1–9.

Harris, C.R., **Millman, K.J.**, **van der Walt, S.J.**, **Gommers, R.**, **Virtanen, P.**, **Cournapeau, D. *et al.*** (2020) Array programming with NumPy. *Nature*, **585**(7825), 357–362. Available from: https://doi.org/10.1038/s41586020-2649-2

Hodac, L., **Barke, B.** & **Hörandl, E.** (2018) Mendelian segregation of leaf phenotypes in experimental F_2 hybrids elucidates origin of morphological diversity of the apomictic *Ranunculus auricomus* complex. *Taxon*, **67**, 6–1092. Available from: https://doi.org/10.12705/676.6

Hodac, L., **Karbstein, K.**, **Tomasello, S.**, **Wäldchen, J.**, **Bradican, J.P.** & **Hörandl, E.** (2023) Geometric morphometric versus genomic patterns in a large polyploid plant species complex. *Biology*, **12**(3), 418. Available from: https://doi.org/10.3390/biology12030418

Holzinger, A., **Saranti, A.**, **Molnar, C.**, **Biecek, P.** & **Samek, W.** (2022) Explainable AI methods—a brief overview. In: *xxAI—beyond explainable AI*. Cham: Springer. Available from: https://doi.org/10.1007/978-3-031-04083-22

Hörandl, E. & **Gutermann, W.** (1995) Die Bearbeitung Der *Ranunculus auricomus*-Gruppe für die Flora von Osterreich "–Ein Werkstattbericht". *Florae Austriacae Novitates*, **2**, 12–27.

Hunter, J.D. (2007) Matplotlib: a 2D graphics environment. *Computing in Science & Engineering*, **9**(3), 90–95. Available from: https://doi.org/10.1109/MCSE.2007.55

Jolliffe, I.T. (2002) *Principal component analysis for special types of data*. New York: Springer.

Jombart, T. (2008) Adegenet: a R package for the multivariate analysis of genetic markers. *Bioinformatics*, **24**(11), 1403–1405. Available from: https://doi.org/10.1093/bioinformatics/btn129

Jombart, T., **Devillard, S.** & **Balloux, F.** (2010) Discriminant analysis of principal components: a new method for the analysis of genetically structured populations. *BMC Genetics*, **11**(1), 94. Available from: https://doi.org/10.1186/1471-2156-11-94

Karbstein, K., **Hodac, L.**, **Wäldchen, J.**, **Tomasello, S.**, **Bradican, J.P.** & **Hörandl, E.** (2023) Geometric morphometric versus genomic patterns in a large polyploid plant species complex. *Figshare*. Available from: https://doi.org/10.6084/m9.figshare.21393375.v1

Karbstein, K., **Kösters, L.**, **Hodač, L.**, **Hofmann, M.**, **Hörandl, E.**, **Tomasello, S.** ***et al.*** (2024) Species delimitation 4.0: integrative taxonomy meets artificial intelligence. *Trends in Ecology & Evolution*, **39**, 771–784. Available from: https://doi.org/10.1016/j.tree.2023.11.002

Karbstein, K., **Tomasello, S.**, **Hodac, L.**, **Daubert, M.**, **Dunkel, F.** & **Hörandl, E.** (2020) Phylogenomics supported by geometric morphometrics reveals delimitation of sexual species within the Polyploid apomictic *Ranunculus auricomus* complex. *Taxon*, **69**, 1191–1220. Available from: https://doi.org/10.1002/tax.12365

Karbstein, K., **Tomasello, S.**, **Hodac, L.**, **Lorberg, E.**, **Daubert, M.** & **Hörandl, E.** (2021) Moving beyond assumptions: polyploidy and environmental effects explain a geographical parthenogenesis scenario in European plants. *Molecular Ecology*, **30**, 2659–2675. Available from: https://doi.org/10.1111/mec.15919

Karbstein, K., **Tomasello, S.**, **Hodac, L.**, **Wagner, N.**, **Marincek, P.**, **Barke, B.H.** ***et al.*** (2022) Untying Gordian knots: unraveling reticulate polyploid plant evolution by genomic data using the large *Ranunculus auricomus* species complex. *New Phytologist*, **235**(5), 2081–2098. Available from: https://doi.org/10.1111/nph.18284

Kayhan, G. (2022) Comparison of the performance of different learning algorithms in leaf feature extraction and recognition using convolution neural network. *Concurrency and Computation: Practice and Experience*, **34**(26), e7294. Available from: https://doi.org/10.1002/cpe.7294

Kiel, S. (2021) Assessing bivalve phylogeny using deep learning and computer vision approaches. *bioRxiv*. Available from: https://doi.org/10.1101/2021.04.08.438943

Klingenberg, C.P. (2011) MorphoJ: an integrated software package for geometric morphometrics. *Molecular Ecology Resources*, **11**(2), 353–357. Available from: https://doi.org/10.1111/j.17550998.2010.02924.x

Klingenberg, C.P. (2013) Visualizations in geometric morphometrics: how to read and how to make graphs showing shape changes. *Hystrix, the Italian Journal of Mammalogy*, **24**(1), 15. Available from: https://doi.org/10.4404/hystrix-24.1-7691

Laga, H., **Kurtek, S.**, **Srivastava, A.** & **Miklavcic, S.J.** (2013) Statistical shape models of plant leaves. In: 2013 *IEEE international conference on image processing*. pp. 3503–3507. Available from: https://doi.org/10.1109/ICIP.2013.6738723

Laga, H., **Kurtek, S.**, **Srivastava, A.** & **Miklavcic, S.J.** (2014) Landmark-free statistical analysis of the shape of plant leaves. *Journal of Theoretical Biology*, **363**, 41–52. Available from: https://doi.org/10.1016/j.jtbi.2014.07.036

Le, V.-L., **Beurton-Aimar, M.**, **Zemmari, A.**, **Marie, A.** & **Parisey, N.** (2020) Automated landmarking for insects morphometric analysis using deep neural networks. *Ecological Informatics*, **60**, 101175. Available from: https://doi.org/10.1016/j.ecoinf.2020.101175

Lee, S.H., **Chan, C.S.**, **Mayo, S.J.** & **Remagnino, P.** (2017) How deep learning extracts and learns leaf features for plant classification. *Pattern Recognition*, **71**, 1–13. Available from: https://doi.org/10.1016/j.patcog.2017.05.015

Li, L., **Wang, Y.**, **Jin, S.**, **Li, M.**, **Chen, Q.**, **Ning, J.** ***et al.*** (2021) Evaluation of black tea by using smartphone imaging coupled with micro-near-infrared spectrometer. *Spectrochimica Acta Part A: Molecular and Biomolecular Spectroscopy*, **246**, 118991. Available from: https://doi.org/10.1016/j.saa.2020.118991

Li, X., **Xiong, H.**, **Li, X.**, **Wu, X.**, **Zhang, X.**, **Liu, J.** ***et al.*** (2022) Interpretable deep learning: interpretation, interpretability, trustworthiness, and beyond. *Knowledge and Information Systems*, **64**(12), 3197–3234. Available from: https://doi.org/10.1007/s10115-02201756-8

Liu, L., **Yu, L.**, **Wu, D.**, **Ye, J.**, **Feng, H.**, **Liu, Q.** ***et al.*** (2021) PocketMaize: an android-smartphone application for maize plant phenotyping. *Frontiers in Plant Science*, **12**, 770217. Available from: https://doi.org/10.3389/fpls.2021.770217

Luong, Y., **Gasca-Herrera, A.**, **Misiewicz, T.M.** & **Carter, B.E.** (2023) A pipeline for the rapid collection of color data from photographs. *Applications in Plant Sciences*, **11**(5), e11546. Available from: https://doi.org/10.1002/aps3.11546

Mäder, P., **Boho, D.**, **Rzanny, M.**, **Seeland, M.**, **Wittich, H.C.**, **Deggelmann, A.** ***et al.*** (2021) The flora incognita app—interactive plant species identification. *Methods in Ecology and Evolution*, **12**(7), 1335–1342. Available from: https://doi.org/10.1111/2041-210X.13611

Mahin, M.R.H., **Moonwar, W.**, **Chy, M.S.R.**, **Rafi, F.F.**, **Shahriar, M.F.**, **Karim, D.Z.** ***et al.*** (2022) Interpretable disease classification in plant leaves using deep convolutional neural networks. In: *International conference on computer and information technology (ICCIT)*. pp, 645–650. Available from: https://doi.org/10.1109/ICCIT57492.2022.10055126

McInnes, L., **Healy, J.**, **Saul, N.** & **Großberger, L.** (2018) UMAP: uniform manifold approximation and projection. *Journal of Open Source Software*, **3**(29), 861. Available from: https://doi.org/10.21105/joss.00861

Melzheimer, V. & **Hörandl, E.** (2022) *Die Ranunculaceae der Flora von Zentraleuropa: Ranunculus sect. auricomus*. Gesellschaft zur Erforschung der Flora Deutschlands e.V. Available from: https://doi.org/10.21248/gups.68734

Milošević, D., **Milosavljević, A.**, **Predić, B.**, **Medeiros, A.S.**, **Savić-Zdravković, D.**, **Stojković Piperac, M.** ***et al.*** (2020) Application of deep learning in aquatic bioassessment: towards automated identification of non-biting midges. *Science of the Total Environment*, **711**, 135160. Available from: https://doi.org/10.1016/j.scitotenv.2019.135160

Mostafa, S., **Mondal, D.**, **Panjvani, K.**, **Kochian, L.** & **Stavness, I.** (2023) Explainable deep learning in plant phenotyping. *Frontiers in Artificial Intelligence*, **6**, 1203546. Available from: https://doi.org/10.3389/frai.2023.1203546

Müller-Linow, M., **Wilhelm, J.**, **Briese, C.**, **Wojciechowski, T.**, **Schurr, U.** & **Fiorani, F.** (2019) Plant screen mobile: an open-source mobile device app for plant trait analysis. *Plant Methods*, **15**(1), 2. Available from: https://doi.org/10.1186/s13007-019-0386-z

Nahiduzzaman, M., **Chowdhury, M.E.H.**, **Salam, A.**, **Nahid, E.**, **Ahmed, F.**, **AlEmadi, N.** ***et al.*** (2023) Explainable deep learning model for automatic mulberry leaf disease classification. *Frontiers in Plant Science*, **14**, 1175515. Available from: https://doi.org/10.3389/fpls.2023.1175515

Nery, E.K. & **Fiaschi, P.** (2019) Geometric morphometrics dismiss the polymorphic *Hydrocotyle quinqueloba* (Araliaceae) from the Neotropics. *Systematic Botany*, **44**(2), 451–469. Available from: https://doi.org/10.1600/036364419X15561132273558

Nguyen, H.H., **Ho, B.H.**, **Lai, H.P.**, **Tran, H.T.**, **Bañuls, A.L.**, **Prudhomme, J.** ***et al.*** (2022) A lightweight keypoint matching framework for insect wing morphometric landmark detection. *Ecological Informatics*, **70**, 101694. Available from: https://doi.org/10.1016/j.ecoinf.2022.101694

Noviandy, T.R., **Maulana, A.**, **Khowarizmi, F.** & **Muchtar, K.** (2023) Effect of CLAHEbased enhancement on bean leaf disease classification through explainable AI. In: 2023 IEEE 12th global conference on consumer electronics (GCCE). pp. 515–516. Available from: https://doi.org/10.1109/GCCE59613.2023.10315394

Ott, T. & **Lautenschlager, U.** (2022) GinJinn2: object detection and segmentation for ecology and evolution. *Methods in Ecology and Evolution*, **13**(3), 603–610. Available from: https://doi.org/10.1111/2041-210X.13787

Paul, H., **Ghatak, S.**, **Chakraborty, S.**, **Pandey, S.K.**, **Dey, L.**, **Show, D.** ***et al.*** (2023) A study and comparison of deep learning based potato leaf disease detection and classification techniques using explainable AI. *Multimedia Tools and Applications*, **83**, 42485–42518. Available from: https://doi.org/10.1007/s11042-023-17235-3

Pedregosa, F., **Varoquaux, G.**, **Gramfort, A.**, **Michel, V.**, **Thirion, B.**, **Grisel, O.** ***et al.*** (2011) Scikit-learn: machine learning in python. *Journal of Machine Learning Research*, **12**, 2825–2830.

Perez-Udell, R.A., **Udell, A.T.** & **Chang, S.-M.** (2023) An automated pipeline for supervised classification of petal color from citizen science photographs. *Applications in Plant Sciences*, **11**(1), e11505. Available from: https://doi.org/10.1002/aps3.11505

Petrović, A., **Mitrović, M.**, **Ivanović, A.**, **Zikić, V.**, **Kavallieratos, N.G.**, **Starý, P.** ***et al.*** (2015) Genetic and morphological variation in sexual and asexual parasitoids of the genus Lysiphlebus—an apparent link between wing shape and reproductive mode. *BMC Evolutionary Biology*, **15**(1), 5. Available from: https://doi.org/10.1186/s12862-015-0293-5

Pinho, C., **Kaliontzopoulou, A.**, **Ferreira, C.A.** & **Gama, J.** (2023) Identification of morphologically cryptic species with computer vision models: wall lizards (Squamata: Lacertidae: *Podarcis*) as a case study. *Zoological Journal of the Linnean Society*, **198**(1), 184–201. Available from: https://doi.org/10.1093/zoolinnean/zlac087

Porto, A., **Rolfe, S.** & **Maga, A.M.** (2021) ALPACA: a fast and accurate computer vision approach for automated landmarking of three-dimensional biological structures. *Methods in Ecology and Evolution*, **12**(11), 2129–2144. Available from: https://doi.org/10.1111/2041-210X.13689

Porto, A. & **Voje, K.L.** (2020) ML-morph: a fast, accurate and general approach for automated detection and landmarking of biological structures in images. *Methods in Ecology and Evolution*, **11**(4), 500–512. Available from: https://doi.org/10.1111/2041-210X.13373

Qi, M., **Du, F.K.**, **Guo, F.**, **Yin, K.** & **Tang, J.** (2024) Species identification through deep learning and geometrical morphology in oaks (*Quercus* Spp.): pros and cons. *Ecology and Evolution*, **14**(2), e11032. Available from: https://doi.org/10.1002/ece3.11032

R Core Team. (2022) *R: a language and environment for statistical computing*. Vienna: R Core Team. https://cran.r-project.org

Reich, D., **Berger, A.**, **von Balthazar, M.**, **Chartier, M.**, **Sherafati, M.**, **Schönenberger, J.** ***et al.*** (2020) Modularity and evolution of flower shape: the role of function, development, and spandrels in Erica. *New Phytologist*, **226**(1), 267–280. Available from: https://doi.org/10.1111/nph.16337

Rodrigues, P.J., **Gomes, W.** & **Pinto, M.A.** (2022) DeepWings©: automatic wing geometric morphometrics classification of honey bee (*Apis mellifera*) subspecies using deep learning for detecting landmarks. *Big Data and Cognitive Computing*, **6**(3), 70. Available from: https://doi.org/10.3390/bdcc6030070

Rohlf, F.J. (2015) The Tps series of software. *Hystrix, the Italian Journal of Mammalogy*, **26**(1), 9–12. Available from: https://doi.org/10.4404/hystrix-26.1-11264

Rueden, C.T., **Schindelin, J.**, **Hiner, M.C.**, **DeZonia, B.E.**, **Walter, A.E.**, **Arena, E.T.** ***et al.*** (2017) ImageJ2: ImageJ for the next generation of scientific image data. *BMC Bioinformatics*, **18**(1), 529. Available from: https://doi.org/10.1186/s12859-017-1934-z

Rzanny, M., **Mäder, P.**, **Deggelmann, A.**, **Chen, M.** & **Wäldchen, J.** (2019) Flowers, leaves or both? How to obtain suitable images for automated plant identification. *Plant Methods*, **15**(1), 77. Available from: https://doi.org/10.1186/s13007-019-0462-4

Rzanny, M., **Seeland, M.**, **Wäldchen, J.** & **Mäder, P.** (2017) Acquiring and preprocessing leaf images for automated plant identification: understanding the tradeoff between effort and information gain. *Plant Methods*, **13**(1), 97. Available from: https://doi.org/10.1186/s13007-017-0245-8

Rzanny, M., **Wittich, H.**, **Mäder, P.**, **Deggelmann, A.**, **Boho, D.** & **Wäldchen, J.** (2022) Image-based automated recognition of 31 poaceae species: the most relevant perspectives. *Frontiers in Plant Science*, **12**, 804140. Available from: https://doi.org/10.3389/fpls.2021.804140

Saleem, G., **Akhtar, M.**, **Ahmed, N.** & **Qureshi, W.S.** (2019) Automated analysis of visual leaf shape features for plant classification. *Computers and Electronics in Agriculture*, **157**, 270–280. Available from: https://doi.org/10.1016/j.compag.2018.12.038

Samek, W., **Montavon, G.**, **Lapuschkin, S.**, **Anders, C.J.** & **Muller, K.-R.** (2021) Explaining deep neural networks and beyond: a review of methods and applications. *Proceedings of the IEEE*, **109**(3), 247–278. Available from: https://doi.org/10.1109/JPROC.2021.3060483

Sano, T. & **Kawabata, H.** (2023) A computational approach to investigating facial attractiveness factors using geometric morphometric analysis and deep learning. *Scientific Reports*, **13**(1), 19797. Available from: https://doi.org/10.1038/s41598-023-47084-x

Savriama, Y. (2018) A step-by-step guide for geometric morphometrics of floral symmetry. *Frontiers in Plant Science*, **9**, 1433. Available from: https://doi.org/10.3389/fpls.2018.01433

Selvaraju, R.R., **Cogswell, M.**, **Das, A.**, **Vedantam, R.**, **Parikh, D.** & **Batra, D.** (2020) Grad-CAM: visual explanations from deep networks via gradient-based localization. *International Journal of Computer Vision*, **128**(2), 336–359. Available from: https://doi.org/10.1007/s11263-01901228-7

Shuai, L., **Mu, J.**, **Jiang, X.**, **Chen, P.**, **Zhang, B.**, **Li, H.** ***et al.*** (2023) An improved YOLOv5-based method for multi-species tea shoot detection and picking point location in complex backgrounds. *Biosystems Engineering*, **231**, 117–132. Available from: https://doi.org/10.1016/j.biosystemseng.2023.06.007

Song, L., **Hong, C.**, **Gao, T.** & **Yu, J.** (2024) Lightweight facial landmark detection network based on improved MobileViT. *Signal, Image and Video Processing*, **18**, 3123–3131. Available from: https://doi.org/10.1007/s11760-023-02975-4

Stojnić, S., **Viscosi, V.**, **Marković, M.**, **Ivanković, M.**, **Orlović, S.**, **Tognetti, R.** ***et al.*** (2022) Spatial patterns of leaf shape variation in European beech (*Fagus sylvatica* L.) provenances. *Trees*, **36**(1), 497–511. Available from: https://doi.org/10.1007/s00468021-02224-6

Stuessy, T.F. (2009) *Plant taxonomy: the systematic evaluation of comparative data*, 2nd edition. New York: Columbia University Press.

Sun, T., **Xue, C.**, **Chen, Y.**, **Zhao, L.**, **Qiao, C.**, **Huang, A.** ***et al.*** (2023) Cost-effective identification of the field maturity of tobacco leaves based on deep semi-supervised active learning and smartphone photograph. *Computers and Electronics in Agriculture*, **215**, 108373. Available from: https://doi.org/10.1016/j.compag.2023.108373

Tan, J., **Wei, S.-W.C.**, **Abdul-Kareem, S.**, **Yap, H.J.** & **Yong, K.-T.** (2020) Deep learning for plant species classification using leaf vein morphometric. *IEEE/ACM Transactions on Computational Biology and Bioinformatics*, **17**(1), 82–90. Available from: https://doi.org/10.1109/TCBB.2018.2848653

Tan, R., **Gao, L.**, **Khan, N.** & **Guan, L.** (2022) Interpretable artificial intelligence through locality guided neural networks. *Neural Networks*, **155**, 58–73. Available from: https://doi.org/10.1016/j.neunet.2022.08.009

Toda, Y. & **Okura, F.** (2019) How convolutional neural networks diagnose plant disease. *Plant Phenomics*, **2019**, 9237136. Available from: https://doi.org/10.34133/2019/9237136

Tomaszewski, D. & **Górzkowska, A.** (2016) Is shape of a fresh and dried leaf the same? *PLoS One*, **11**(4), e0153071. Available from: https://doi.org/10.1371/journal.pone.0153071

Virtanen, P., **Gommers, R.**, **Oliphant, T.E.**, **Haberland, M.**, **Reddy, T.**, **Cournapeau, D.** ***et al.*** (2020) SciPy 1.0: fundamental algorithms for scientific computing in python. *Nature Methods*, **17**(3), 261–272. Available from: https://doi.org/10.1038/s41592-019-0686-2

Viscosi, V. & **Cardini, A.** (2011) Leaf morphology, taxonomy and geometric morphometrics: a simplified protocol for beginners. *PLoS One*, **6**(10), e25630. Available from: https://doi.org/10.1371/journal.pone.0025630

Wäldchen, J. & **Mäder, P.** (2018) Plant species identification using computer vision techniques: a systematic literature review. *Archives of Computational Methods in Engineering*, **25**(2), 507–543. Available from: https://doi.org/10.1007/s11831-016-9206-z

Wäldchen, J., **Rzanny, M.**, **Seeland, M.** & **Mäder, P.** (2018) Automated plant species identification—trends and future directions. *PLoS Computational Biology*, **14**(4), e1005993. Available from: https://doi.org/10.1371/journal.pcbi.1005993

Wang, H., **Cheng, R.**, **Zhou, J.**, **Tao, L.** & **Kwan, H.K.** (2022) Multistage model for robust face alignment using deep neural networks. *Cognitive Computation*, **14**(3), 1123–1139. Available from: https://doi.org/10.1007/s12559-021-09846-5

Wöber, W., **Curto, M.**, **Tibihika, P.**, **Meulenbroek, P.**, **Alemayehu, E.**, **Mehnen, L.** ***et al.*** (2021) Identifying geographically differentiated features of Ethopian Nile tilapia (*Oreochromis niloticus*) morphology with machine learning. *PLoS One*, **16**(4), e0249593. Available from: https://doi.org/10.1371/journal.pone.0249593

Wöber, W., **Mehnen, L.**, **Curto, M.**, **Tibihika, P.D.**, **Tesfaye, G.** & **Meimberg, H.** (2022) Investigating shape variation using generalized procrustes analysis and machine learning. *Applied Sciences*, **12**(6), 3158. Available from: https://doi.org/10.3390/app12063158

Woods, C., **Fernee, C.**, **Browne, M.**, **Zakrzewski, S.** & **Dickinson, A.** (2017) The potential of statistical shape modelling for geometric morphometric analysis of human teeth in archaeological research. *PLoS One*, **12**(12), e0186754. Available from: https://doi.org/10.1371/journal.pone.0186754

Wu, Y., **Hipp, A.L.**, **Fargo, G.**, **Stith, N.** & **Ricklefs, R.E.** (2023) Improving species delimitation for effective conservation: a case study in the endemic maple-leaf oak (*Quercus acerifolia*). *New Phytologist*, **238**(3), 1278–1293. Available from: https://doi.org/10.1111/nph.18777

Yang, K., **Zhong, W.** & **Li, F.** (2020) Leaf segmentation and classification with a complicated background using deep learning. *Agronomy*, **10**(11), 1721. Available from: https://doi.org/10.3390/agronomy10111721

Yee, W.L., **Sheets, H.D.** & **Chapman, P.S.** (2011) Analysis of Surstylus and Aculeus shape and size using geometric morphometrics to discriminate *Rhagoletis pomonella* and *Rhagoletis zephyria* (Diptera: Tephritidae). *Annals of the Entomological Society of America*, **104**(2), 105–114. Available from: https://doi.org/10.1603/AN10029

Yun, H.S., **Hyun, C.M.**, **Baek, S.H.**, **Lee, S.-H.** & **Seo, J.K.** (2022) A semi-supervised learning approach for automated 3D cephalometric landmark identification using computed tomography. *PLoS One*, **17**(9), e0275114. Available from: https://doi.org/10.1371/journal.pone.0275114

Zelditch, M.L., **Swiderski, D.L.** & **Sheets, H.D.** (2012) Introduction. In: *Geometric morphometrics for biologists*. Amsterdam: Elsevier, pp. 1–20. Available from: https://doi.org/10.1016/B978-0-12-386903-6.00001-0